Title	Multi-scale analysis of the effect of nano-filler particle diameter on the physical properties of CAD/CAM composite resin blocks
Author(s)	Yamaguchi, Satoshi; Inoue, Sayuri; Sakai, Takahiko et al.
Citation	Computer Methods in Biomechanics and Biomedical Engineering. 2017, 20(7), p. 714-719
Version Type	AM
URL	https://hdl.handle.net/11094/93081
rights	This article is licensed under a Creative Commons Attribution-NonCommercial-NoDerivatives 4.0 International License.
Note	

Research Articles

Multi-scale analysis of the effect of nano-filler particle diameter on the physical properties of CAD/CAM composite resin blocks

Satoshi Yamaguchi[a]*, Sayuri Inoue[a,b], Takahiko Sakai[a], Tomohiro Abe[a], Haruaki Kitagawa[a], Satoshi Imazato[a]

[a] Department of Biomaterials Science, Osaka University Graduate School of Dentistry, 1-8 Yamadaoka, Suita, Osaka 565-0871, Japan

[b] Department of Orthodontics and Dentofacial Orthopedics, Osaka University Graduate School of Dentistry, 1-8 Yamadaoka, Suita, Osaka 565-0871, Japan

* Correspondence should be addressed to Satoshi Yamaguchi

Department of Biomaterials Science, Osaka University Graduate School of Dentistry

1-8 Yamadaoka, Suita, Osaka 565-0871, Japan

Tel/Fax: +81-6-6879-2919

E-mail: yamagu@dent.osaka-u.ac.jp

ABSTRACT

The objective of this study was to assess the effect of silica nano-filler particle diameters in a computer-aided design/manufacturing (CAD/CAM) composite resin (CR) block on physical properties at the multi-scale *in silico*. CAD/CAM CR blocks were modeled, consisting of silica nano-filler particles (20, 40, 60, 80, and 100 nm) and matrix (Bis-GMA/TEGDMA), with filler volume contents of 55.161%. Calculation of Young's moduli and Poisson's ratios for the block at macro-scale were analyzed by homogenization. Macro-scale CAD/CAM CR blocks (3×3×3 mm) were modeled and compressive strengths were defined when the fracture loads exceeded 6075 N. MPS values of the nano-scale models were compared by localization analysis. As the filler size decreased, Young's moduli and compressive strength increased, while Poisson's ratios and MPS decreased. All parameters were significantly correlated with the diameters of the filler particles (Pearson's correlation test, r = −0.949, 0.943, −0.951, 0.976, $p < 0.05$). The *in silico* multi-scale model established in this study demonstrates that the Young's moduli, Poisson's ratios, and compressive strengths of CAD/CAM CR blocks can be enhanced by loading silica nanofiller particles of smaller diameter. CAD/CAM CR blocks by using smaller silica nano-filler particles have a potential to increase fracture resistance.

KEYWORDS

Composite resins; CAD/CAM; multi-scale analysis; compressive strength; maximum principal strain

1 INTRODUCTION

Computer-aided design/computer-aided manufacturing (CAD/CAM) composite resin (CR) blocks containing a high density of nano-filler particles (Nguyen et al. 2012, Nguyen et al. 2013, Okada et al. 2014) have been available for posterior restorations (Lauvahutanon et al. 2014, Shembish et al. 2016). In comparison with conventional CRs (Ferracane 2011, Ilie and Hickel 2009), CAD/CAM CR blocks exhibit superior mechanical properties, such as flexural strength, Vickers hardness, and fracture toughness in terms of their clinical wear performance (Thomaidis et al. 2013). Although Vickers hardness values are lower than those of ceramics, flexural strength is comparable to that of a ceramic block and within the acceptable range (>100 MPa) for single restorations described in the ISO standard for ceramic dental implants (Lauvahutanon, Takahashi, Shiozawa, Iwasaki, Asakawa, Oki, Finger and Arksornnukit 2014). In addition, the effect of compressive cyclic loading on fatigue resistance of CAD/CAM CR crowns has been investigated and there is no greater incidence of catastrophic failure and lower microleakage compared with ceramic crowns (Kassem et al. 2012). These results suggest that greater compressive strength possibly improves the fatigue resistance of CAD/CAM CR crowns.

In conventional CRs, the Young’s moduli measured by the nanoindentation test increases as the average diameter of filler particles increases at constant volume content (Masouras et al. 2008). To further improve the mechanical properties of CAD/CAM CR blocks and achieve excellent clinical wear performance, optimization of the size of nano-filler particles is required. However, the influence of nano-filler size on the compressive strength of CAD/CAM CR blocks cannot be rigorously evaluated through *in vitro* testing, because the average diameter of nano-fillers is not controllable in experimental CRs, and crack initiations at the nano-scale during fatigue testing cannot be followed even by observation with scanning electron microscopy (Shembish, Tong, Kaizer, Janal, Thompson, Opdam and Zhang 2016).

In silico analysis combined with three-dimensional finite element analysis and composite theory has been useful for evaluating specific differences, such as the volume content of fillers in conventional CRs (Li et al. 2012). However, the controllable parameter for *in silico* analysis has been limited to date to the volume content, and excludes the size of the fillers.

In silico multi-scale analysis (**Fig. 1**) is a coupled method for analysis of physical properties or behaviors between different scales that has been used to predict mechanical properties of composite materials (Guedes and Kikuchi 1990) and has been applied to the prediction of mechanical strength of porous ceramics (Takano et al. 2003) and titanium

(Takano et al. 2010). This approach consists of homogenization analysis and localization analysis. Homogenization analysis is a method for obtaining physical properties at the macro-scale from knowledge of nano- or micro-scale structures. Nano- or micro-scale stress and strain distribution for each component material in composite materials can be visualized by localization analysis. This multi-scale approach enables the investigation of the influence of nano-filler particle size on the physical properties at the macro-scale.

The objective of this study was to assess the effect of silica nano-filler particle diameter in CAD/CAM CR blocks on the Young's modulus, Poisson's ratio, and compressive strength at the macro-scale, and the maximum principal strain (MPS) at the nano-scale through *in silico* multi-scale analysis.

2. MATERIALS AND METHODS

2.1. *In silico* models

Nano-scale CAD/CAM CR block models were designed using CAD software (Solidworks Simulation 2011, Dassault Systèmes SoldWorks Corporation, Massachusetts, USA), consisting of silica nano-filler particles (20, 40, 60, 80, and 100 nm) and matrix (Bis-GMA/TEGDMA) (45×45×45, 90×90×90, 135×135×135, 180×180×180 and 225×225×225 nm), with filler volume contents of 55.161% (**Fig. 2**). The material properties of silica and Bis-GMA/TEGDMA are shown in **Table 1**.

2.2. Homogenization analysis

A macro-scale CAD/CAM CR block model (3×3×3 mm) was designed by Solidworks Simulation 2011 (**Fig. 3**) for compressive analysis. Calculation of Young's moduli and Poisson's ratios for the block were conducted by homogenization analysis in computer-aided engineering software (VOXELCON2015, Quint Corporation., Fuchu, JAPAN). Compressive strengths were defined as the values when the fracture loads exceeded 6075 N. The MPS distribution in the macro-scale model was observed and normal strains in x-, y-, and z-axes and shear strains in yz-, zx-, and xy-planes were recorded at the location of the maximum MPS value.

2.3. Localization analysis

The MPS distribution in nano-scale models at the location where the maximum MPS values were obtained in the macro-scale model was examined by localization analysis (VOXELCON2015). The maximum MPS values at the nano-scale, related to the threshold of fracture initiation, were compared.

2.4. Statistical analysis

All parameters were statistically analyzed using Pearson's correlation test (PASW Statistics 18, IBM, New York, USA).

3. RESULTS

3.1. Homogenization analysis

Young's moduli, Poisson's ratios, and compressive strengths at the macro-scale are shown in Table 2. The results of macro-scale analyses show that the maximum MPS values were observed at the vertex of the top surface of the cube (**Fig. 4**). As the filler diameter decreased, Young's moduli and compressive strengths increased (**Fig 5a** and **5c**), while Poisson's ratios decreased (**Fig 5b**).

3.2. Localization analysis

Maximum MPS values at the nano-scale containing 20-, 40-, 60-, 80-, and 100-nm filler particles are shown in Table 2. As the filler diameter decreased, the maximum MPS values decreased (**Fig. 5d**). The maximum MPS values were observed in the matrix resins at the nano-filler particle spacing (**Fig. 6**). The nano-scale model containing 20-nm filler particles showed the lowest concentration of MPS values compared with the other models (**Fig. 6a**).

3.3. Statistical analysis

All parameters were significantly correlated with the diameters of filler particles (Pearson's correlation test, r = -0.949, 0.943, -0.951, 0.976, $p < 0.05$).

4. DISCUSSION

By comparing the maximum MPS values amongst the nano-scale models at the location where the maximum MPS values were obtained at the macro-scale, the model with the greatest compressive strength was identified under the assumption of the following MPS theory (Hearn 1997). MPS has been used as a failure criterion for the matrix in fiber-reinforced composites during *in silico* analysis, resulting in good agreement with experimental results (Hoover et al. 1997, Xia et al. 2000). Our results are the first report describing the investigation of MPS propagation in nano-scale filler particles and the resin matrix to elucidate the detailed mechanism behind compressive strength. The *in silico* multi-scale analysis used in this study is useful for understanding detailed stress and strain distributions at the nano-scale, which is not possible through *in vitro* testing, and is applicable to the investigation of the influence of other controllable parameters such as geometric shape and the spatial layout of nano-filler particles.

With regard to the homogenization analyses, Young's moduli showed a 28.131% increase of the nano-scale model containing 100-nm filler particles compared with that containing 20-nm filler particles, while Poisson's ratios decreased 10.619% at the same volume content. The relationship between Young's moduli and Poisson's ratio was comparable with that for conventional CRs (Masouras, Akhtar, Watts and Silikas 2008).

Young's moduli of conventional CRs increase, while their Poisson's ratios decrease, as the filler fraction increases (Li, Li, Fok and Watts 2012). However, the preparation of CRs with high filler fractions is difficult because of theoretical limitations. In the case of face-centered cubic lattice and hexagonal close packing structures using uniformly sized sphere filler particles, the theoretical maximum content of particles is 74 vol% (Sloane 2003). The maximum filler content found for 72 commercial composites was 70 vol% (Ilie and Hickel 2009). Higher filler contents induce lower fatigue resistance (Htang et al. 1995). Our results suggest that CRs with small, spherical nano-filler particles have the potential to improve the Young's modulus and Poisson's ratio even at lower filler fractions such as 55.161%, used in this study. Compressive strengths increased by 31.010% in a nano-scale model containing 20-nm filler particles from that containing 100-nm filler particles, while the maximum MPS values were decreased by 71.413%. Under the same amount of loading, lower values of the maximum MPS definitely showed greater compressive strength because the maximum MPS is defined as the threshold required to initiate compressive fracture. These results suggest that the compressive strength of CAD/CAM CR blocks with constant volume content can be improved by using smaller filler particles.

With regard to the localization analysis, the model containing 20-nm filler particles showed the lowest maximum MPS at the nano-scale and must have the greatest total surface area of filler particles at the same volume content compared with the other models. This phenomenon, called the “nano-effect”, induces an enormous interfacial area per unit volume (Fiedler et al. 2006, Wichmann et al. 2006) and the silane coupling rate increases in association with the increase in the total surface area of filler particles. Although there is a lack of simulation for the silane coupling ratio between silica nano-filler particles and matrix resins (Tanimoto et al. 2006), the physical properties of CAD/CAM CR blocks obtained in this study were identified, with the exception of the relative decrease in absolute values associated with failure rates of the silane coupling. In addition, uniformly dispersed, smaller nano-filler particles contribute to energy absorption and dissipation through the nano-effect (Opelt et al. 2015). The propagation of elastic waves on human tooth enamel has been analyzed by the time-dependent finite element method and moving particle simulation (Yamaguchi et al. 2014). This approach is applicable to evaluate the performance of energy absorption and dissipation in CAD/CAM CR blocks, while a static analysis was used in this study.

Further fatigue testing to evaluate the long-term performance of CAD/CAM CR crowns has also been required (Harada et al. 2015). High fracture resistance of a mandibular first molar crown fabricated by Lava Ultimate then IPS Empress CAD has been reported (Shembish, Tong, Kaizer, Janal, Thompson, Opdam and Zhang 2016) and fabrication of other crowns by commercial CAD/CAM CR blocks are ongoing for investigating the relationship between compressive strength and fatigue resistance. In addition, *in silico* probabilistic fatigue analyses of all-ceramic crowns have been proposed (Lekesiz 2014, Zhang et al. 2010) and may have potential as a useful approach for predicting the reliability of CAD/CAM CR crowns, while long-term *in vivo* trials to investigate clinical performance have been eagerly anticipated (Ruse and Sadoun 2014, Shembish, Tong, Kaizer, Janal, Thompson, Opdam and Zhang 2016).

5. CONCLUSIONS

The *in silico* multi-scale model established in this study demonstrated that the Young's moduli, Poisson's ratios, and compressive strengths of CAD/CAM CR blocks can be enhanced by loading silica nano-filler particles of smaller diameter. CAD/CAM CR blocks by using smaller silica nano-filler particles have a potential to increase fracture resistance.

ACKNOWLEDGEMENT

This research was supported by a Grant-in-Aid for Scientific Research (No. JP15K11195) from the Japan Society for the Promotion of Science (JSPS).

References

Ferracane JL. 2011. Resin composite--state of the art. Dent Mater. 27:29-38.

Fiedler B, Gojny FH, Wichmann MHG, Nolte MCM, Schulte K. 2006. Fundamental aspects of nano-reinforced composites. Compos Sci Technol. 66:3115-3125.

Guedes JM, Kikuchi N. 1990. Preprocessing and Postprocessing for Materials Based on the Homogenization Method with Adaptive Finite-Element Methods. Comput Method Appl M. 83:143-198.

Harada A, Nakamura K, Kanno T, Inagaki R, Ortengren U, Niwano Y, Sasaki K, Egusa H. 2015. Fracture resistance of computer-aided design/computer-aided manufacturing-generated composite resin-based molar crowns. Eur J Oral Sci. 123:122-129.

Hearn EJ. 1997. Mechanics of materials : an introduction to the mechanics of elastic and plastic deformation of solids and structural materials. 3rd ed. Oxford ; Boston: Butterworth-Heinemann. 96049967 //r98

(Edwin John)

E.J. Hearn.

ill. ; 25 cm.

Includes bibliographical references and indexes.

Also available online.

Hoover JW, Kujawski D, Ellyin F. 1997. Transverse cracking of symmetric and unsymmetric glass-fibre/epoxy-resin laminates. Composites Science and Technology.57:1513-1526.

Htang A, Ohsawa M, Matsumoto H. 1995. Fatigue resistance of composite restorations: effect of filler content. Dent Mater. 11:7-13.

Ilie N, Hickel R. 2009. Investigations on mechanical behaviour of dental composites. Clin Oral Investig. 13:427-438.

Kassem AS, Atta O, El-Mowafy O. 2012. Fatigue resistance and microleakage of CAD/CAM ceramic and composite molar crowns. J Prosthodont. 21:28-32.

Lauvahutanon S, Takahashi H, Shiozawa M, Iwasaki N, Asakawa Y, Oki M, Finger WJ, Arksornnukit M. 2014. Mechanical properties of composite resin blocks for CAD/CAM. Dent Mater J.33:705-710.

Lekesiz H. 2014. Reliability estimation for single-unit ceramic crown restorations. J Dent Res. 93:923-928.

Li J, Li H, Fok AS, Watts DC. 2012. Numerical evaluation of bulk material properties of dental composites using two-phase finite element models. Dent Mater. 28:996-1003.

Masouras K, Akhtar R, Watts DC, Silikas N. 2008. Effect of filler size and shape on local nanoindentation modulus of resin-composites. J Mater Sci Mater Med. 19:3561-3566.

Nguyen JF, Migonney V, Ruse ND, Sadoun M. 2012. Resin composite blocks via high-pressure high-temperature polymerization. Dent Mater. 28:529-534.

Nguyen JF, Migonney V, Ruse ND, Sadoun M. 2013. Properties of experimental urethane dimethacrylate-based dental resin composite blocks obtained via thermo-polymerization under high pressure. Dent Mater. 29:535-541.

Okada K, Kameya T, Ishino H, Hayakawa T. 2014. A novel technique for preparing dental CAD/CAM composite resin blocks using the filler press and monomer infiltration method. Dent Mater J.33:203-209.

Opelt CV, Becker D, Lepienski CM, Coelho LAF. 2015. Reinforcement and toughening mechanisms in polymer nanocomposites - Carbon nanotubes and aluminum oxide. Compos Part B-Eng. 75:119-126.

Ruse ND, Sadoun MJ. 2014. Resin-composite blocks for dental CAD/CAM applications. J Dent Res. 93:1232-1234.

Shembish FA, Tong H, Kaizer M, Janal MN, Thompson VP, Opdam NJ, Zhang Y. 2016. Fatigue resistance of CAD/CAM resin composite molar crowns. Dent Mater. 32:499-509.

Sloane N. 2003. Kepler's conjecture: How some of the greatest minds in history helped solve one of the oldest math problems in the world. Nature. 425:126-127.

Takano N, Fukasawa K, Nishiyabu K. 2010. Structural strength prediction for porous titanium based on micro-stress concentration by micro-CT image-based multiscale simulation. Int J Mech Sci. 52:229-235.

Takano N, Zako M, Kubo F, Kimura K. 2003. Microstructure-based stress analysis and evaluation for porous ceramics by homogenization method with digital image-based modeling. Int J Solids Struct. 40:1225-1242.

Tanimoto Y, Kitagawa T, Aida M, Nishiyama N. 2006. Experimental and computational approach for evaluating the mechanical characteristics of dental composite resins with various filler sizes. Acta Biomater. 2:633-639.

Thomaidis S, Kakaboura A, Mueller WD, Zinelis S. 2013. Mechanical properties of contemporary composite resins and their interrelations. Dent

Mater. 29:e132-141.

Wichmann MHG, Cascione M, Fiedler B, Quaresimin M, Schulte K. 2006. Influence of surface treatment on mechanical behaviour of fumed silica/epoxy resin nanocomposites. Compos Interface.13:699-715.

Xia ZH, Chen Y, Ellyin F. 2000. A meso/micro-mechanical model for damage progression in glass-fiber/epoxy cross-ply laminates by finite-element analysis. Compos Sci Technol.60:1171-1179.

Yamaguchi S, Coelho PG, Thompson VP, Tovar N, Yamauchi J, Imazato S. 2014. Dynamic finite element analysis and moving particle simulation of human enamel on a microscale. Comput Biol Med. 55:53-60.

Zhang L, Wang Z, Chen J, Zhou W, Zhang S. 2010. Probabilistic fatigue analysis of all-ceramic crowns based on the finite element method. J Biomech. 43:2321-2326.

Tables

Table 1. Material properties of silica and Bis-GMA/TEGDMA used for homogenization analysis

	Young's modulus (MPa)	Poisson's ratio
Silica	72000	0.16
Bis-GMA/TEGDMA	2000	0.45

Table 2. Physical properties resulting from homogenization and localization analyses

Size of nano-filler particles (nm)	20	40	60	80	100
Young's moduli (GPa)	16.739	15.110	13.814	13.524	13.064
Poisson's ratios	0.303	0.320	0.332	0.335	0.339
Compressive strengths (MPa)	752	675	611	597	574
Maximum MPS	2.652e-3	4.943e-3	7.081e-3	7.340e-3	9.277e-3

Figure Legends

Figure 1. Schematic of multi-scale analysis, consisting of homogenization and localization analyses.

Figure 2. Nano-scale models containing (a) 20-, (b) 40-, (c) 90-, (d) 135- and (e) 180-nm filler particles.

Figure 3. Macro-scale model.

Figure 4. Maximum principal strain distribution in macro-scale models containing (a) 20-, (b) 40-, (c) 90-, (d) 135- and (e) 180-nm filler particles.

Figure 5. Relationship between nano-filler diameters and physical properties resulting from homogenization and localization analysis. (a) Young's modulus, (b) Poisson's ratio, (c) compressive strength, and (d) maximum value of maximum principal strain in nano-scale models.

Figure 6. Maximum principal strain distribution in nano-scale models containing (a) 20-, (b) 40-, (c) 90-, (d) 135- and (e) 180-nm filler particles. Red arrows indicate the locations of maximum values of maximum principal strain observed.

Figure 1

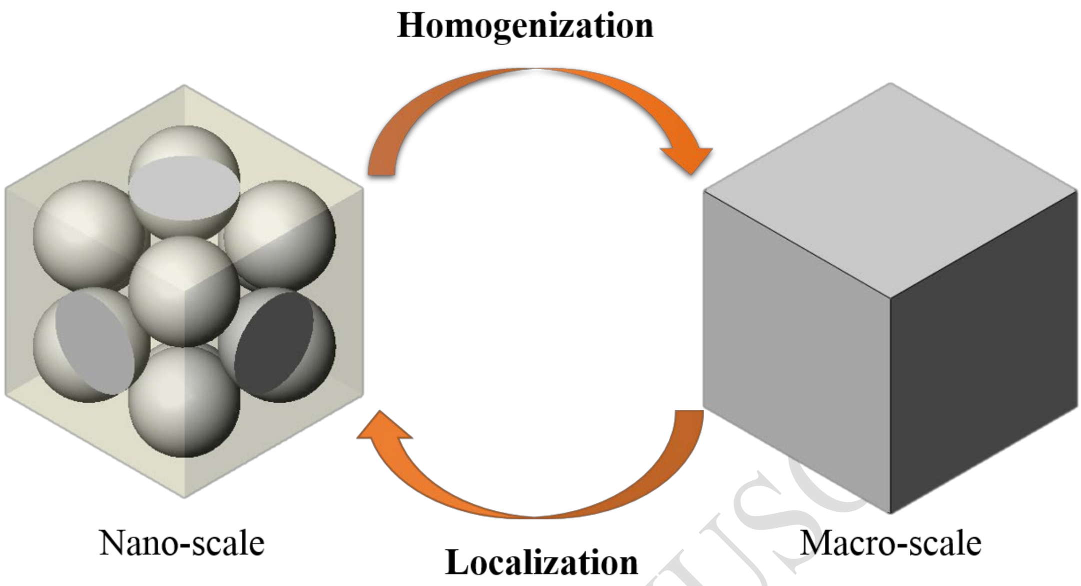

Figure 2

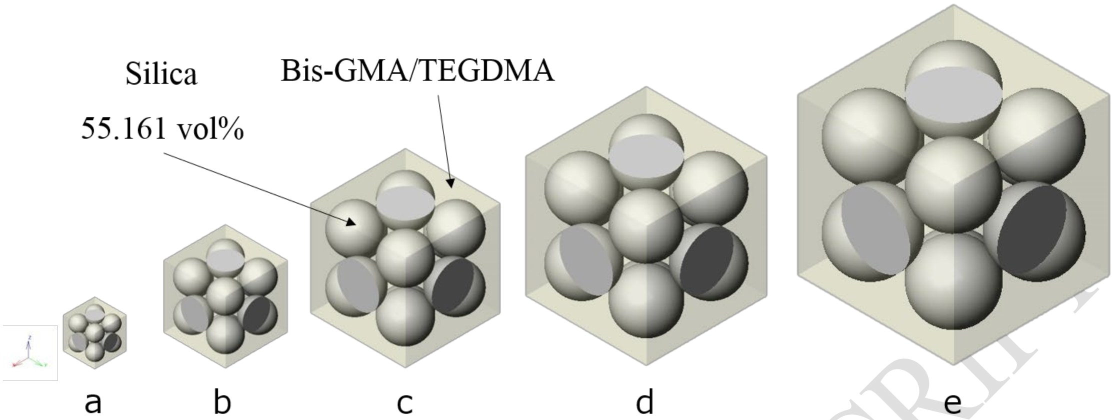

Figure 3

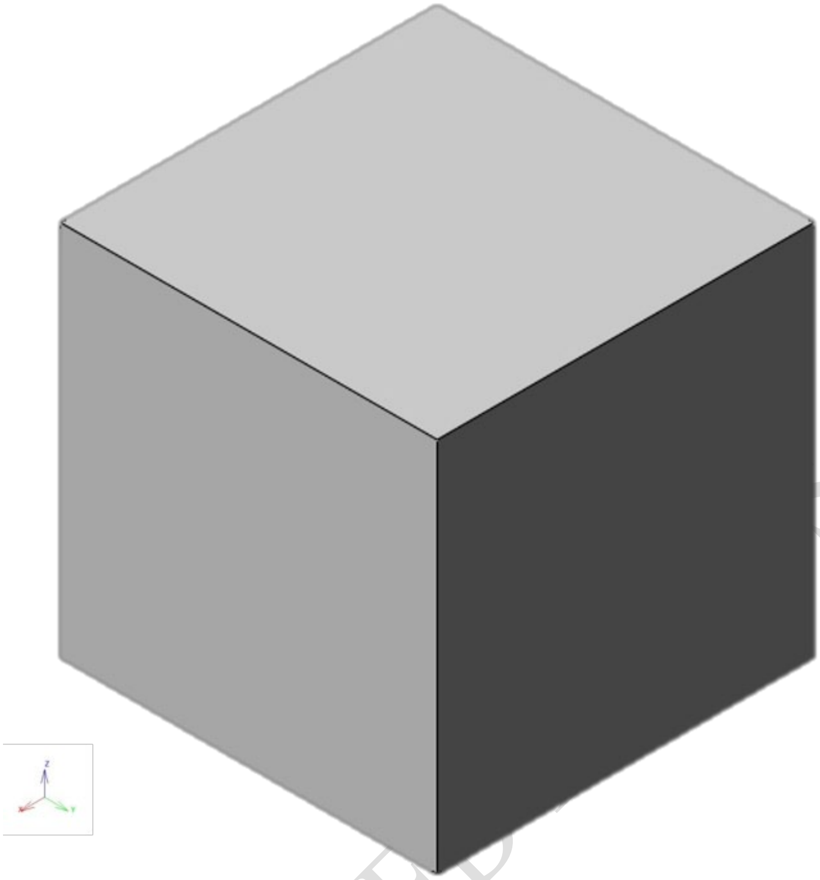

1 Figure 4

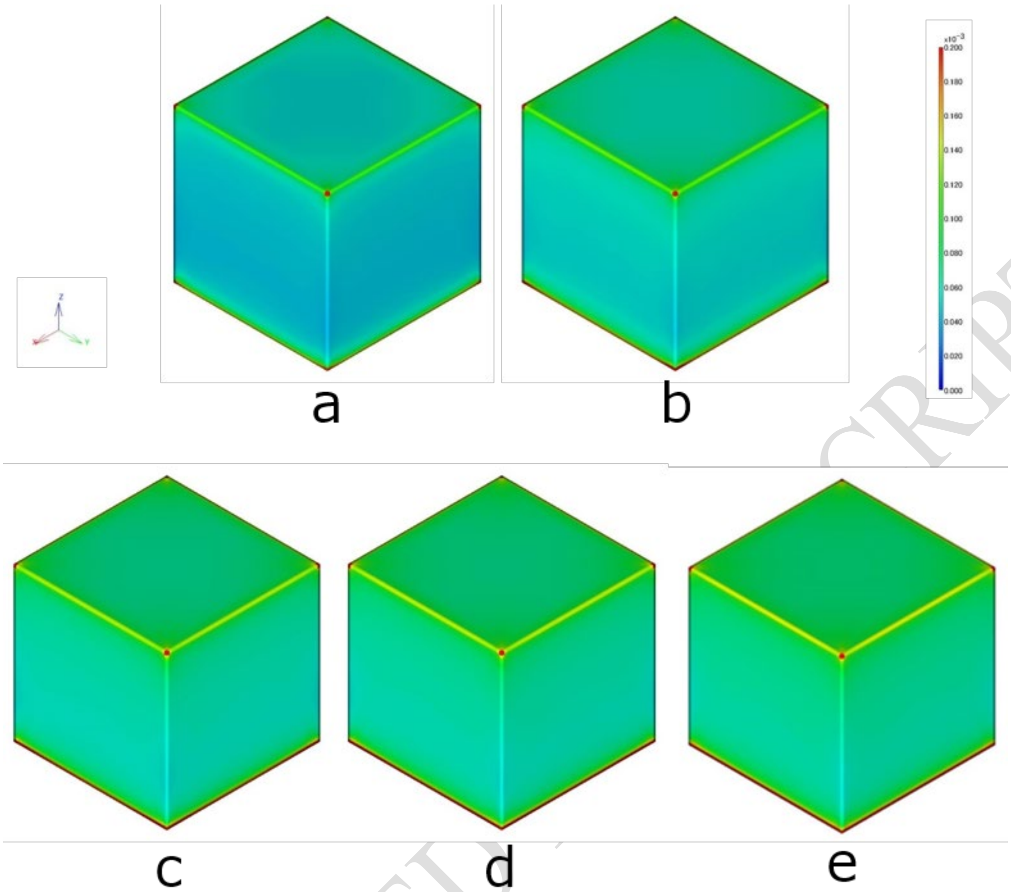

x10^-3
0.200
0.180
0.160
0.140
0.120
0.100
0.080
0.060
0.040
0.020
0.000
a
b
c
d
e

2

3

Figure 5

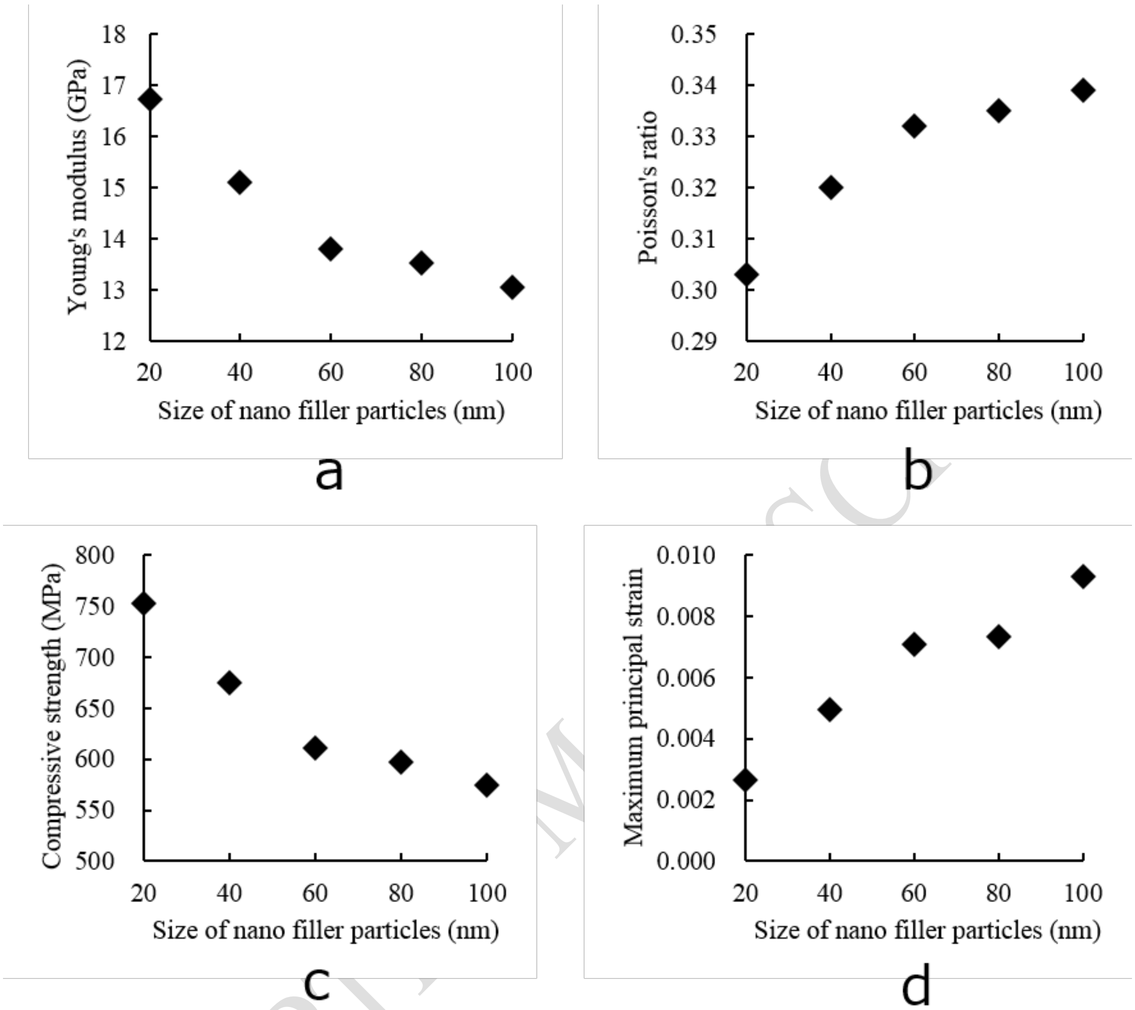
Young's modulus (GPa)
Size of nano filler particles (nm)
a
Poisson's ratio
Size of nano filler particles (nm)
b
Compressive strength (MPa)
Size of nano filler particles (nm)
c
Maximum principal strain
Size of nano filler particles (nm)
d

1 Figure 6

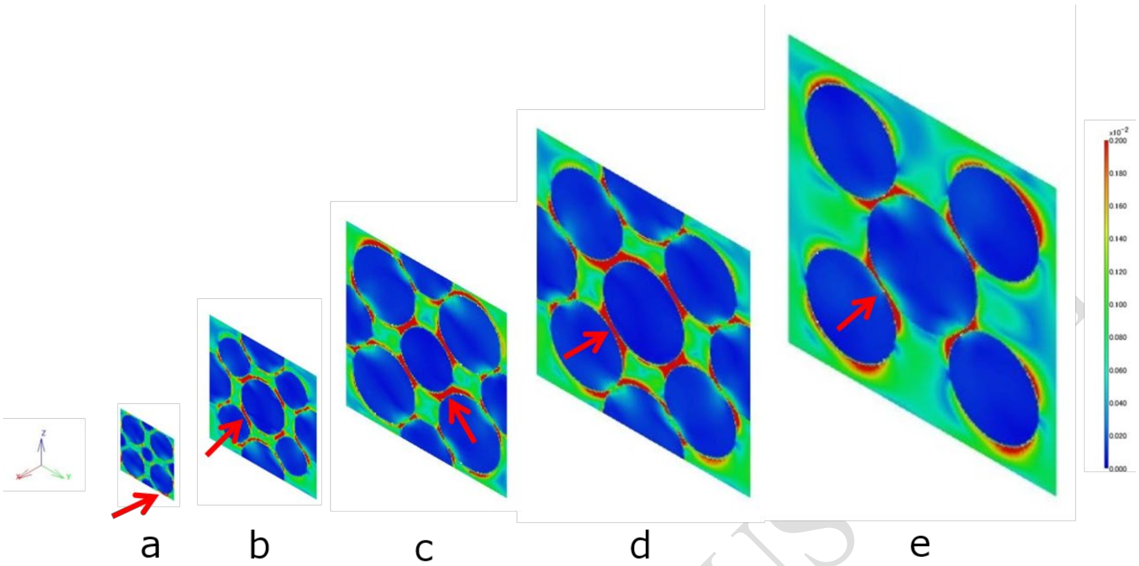

2

3